Production of porous hydroxyapatite by the gel-casting of foams and cytotoxic evaluation

P. Sepulveda,[1]* J.G.P. Binner,[2] S.O. Rogero,[3] O.Z. Higa,[3] J.C. Bressiani[3]**

[1]*Departamento de Engenharia de Materiais, Universidade Federal de São Carlos, Via Washington Luiz, km 235, São Carlos, S.P., 13565-905, Brazil*

[2]*Department of Materials Engineering and Materials Design, University of Nottingham, United Kingdom*

[3]*Instituto de Pesquisas Energéticas e Nucleares, IPEN/CNEN, São Paulo, SP, Brazil*

Received 14 June 1999; accepted 11 August 1999

Abstract: This study presents the manufacture of highly porous hydroxyapatite by a novel technique that employs the foaming of suspensions prior to the *in situ* polymerization of organic monomers contained in the compositions. This method produces strong gelled bodies with up to 90% porosity that can withstand machining in the green state. Complex-shaped components can be obtained if the process comprises casting in one of the processing steps. The organic additives are eliminated at temperatures above 300°C, and sintering is carried out for consolidation of the ceramic matrix. Spherical interconnected cells with sizes ranging from 20 to 1000 μm characterize the porous structure, depending on the specimen density. Cytotoxicity tests were conducted on extracts from sintered HA foams based on a quantitative method of cell colony formation and the determination of cell death after indirect contact of the porous material with mammalian cells. This *in vitro* test of biological evaluation revealed that the original purity of the biomedical-grade hydroxyapatite powder was affected neither through processing nor by the employed reagents. © 2000 John Wiley & Sons, Inc. J Biomed Mater Res, 50, 27–34, 2000.

Key words: porous ceramics; hydroxyapatite; gel-cast foams; cytotoxicity; bone implants

INTRODUCTION

Hydroxyapatite ceramics have been shown to be suitable for biomedical applications, such as bone repair, mainly because of their high biocompatibility, which results from their similarity with the chemical composition of natural bone, $Ca_{10}(PO_4)_6(OH)_2$. Considering this very attractive feature, it would be desirable to reproduce the bone characteristics not only in terms of mineral composition but also in terms of pore morphology. Porous implants allow development of bone and soft tissues within large pores and also blood supply for further bone mineralization. Anchorage between the implant and host bone also is improved by the presence of porosity.[1–4]

In practice, many difficulties arise from attempts to reproduce the pore structure of natural bone. Artificially made porous materials are low in strength and brittle, hence unreliable for structural applications. Consequently, the use of porous ceramics made of hydroxyapatite has been limited mainly to powder, granules, or small dense parts. Materials found in nature, such as graft bone and coral, have provided good alternatives for bone implants although problems related to intrinsic impurities still are a concern.[5]

In the search for stronger porous ceramics, a variety of processing techniques have been developed, including the addition of a fugitive phase material, replication of sponges, foaming, and undersintering, among others. Recently, a novel route to porous ceramics has been reported that enables the maximization of the mechanical strength by introducing macropores in a fully densified matrix. The process combines the gel-casting of ceramics with foaming.[6] Unprecedented high flexural strengths were reported for porous alumina produced in this way, for instance alumina with 70 to 92% porosity revealed values as high as 2 to 26 MPa.[7] Control of pore size and connectivity has been shown to be possible through density variation and expansion of the foams before setting of the foamed slurries.

The present paper describes the processing steps for production of porous bodies from biomedical grade hydroxyapatite. Foaming by the introduction of surfactants and agitation was carried out prior to setting by *in situ* polymerization. The density and pore size

*Present address: Imperial College, Department of Materials, Prince Consort Road, SW7 2BP, London, U.K.

**Present address: Department of Materials Engineering, Brunel University, Uxbridge, UB8 3PH, U.K.

Correspondence to: P. Sepulveda

 CCC 0021-9304/00/010027-08

can be varied accordingly with the amount of foam produced. *In vitro* tests of cytotoxicity were performed on HA foams to verify whether the manipulation of powders and chemical reagents used in the processing can influence the original nontoxicity of HA powder.

MATERIALS AND METHODS

Powder characterization

Hydroxyapatite of biomedical grade CAPTAL-R (Plasma Biotal, UK) was used as the main raw material in this study. High-resolution images of the HA powder were obtained by scanning electron microscopy (SEM) and transmission electron microscopy (TEM). In the latter, sample preparation involved the dispersion of a small quantity of powder into alcohol. With the help of a pipette, the solution was poured onto a 3-mm diameter carbon grid where the solvent was allowed to dry.

Dispersion of hydroxyapatite suspensions

The processing technique used for fabrication of the porous ceramics initially involves the preparation of an aqueous suspension from a mixture of the hydroxyapatite powder, distilled water, dispersing agents, and an organic monomer solution for setting of the slurry. Polyacrylic acid dispersants were used as the dispersing agents for HA, including Versicol KA11 and Dispex A40 (Allied Colloids, Bradford, UK). The aqueous solution of monomers (Allied Colloids, UK) used to set the slips contained approximately 29% acrylate monomers and 1 wt % methylenebisacrylamide monomers. The latter are dienes, introduced to enhance crosslinking by co-polymerization to produce a three-dimensional network of polymers. The monomer content was kept constant in all slips, at approximately 5-6 wt %.

The mixture was homogenized with a polyethylene spatula to avoid contamination. When a uniform mass was formed, mechanical agitation was applied with a single-blade stirrer. Further homogenization was conducted in ball mills, using alumina grinding media, for 15–30 min. Slip de-aeration was achieved by placing the slips in a dessicator for a minimum period of 5 min to remove the dissolved oxygen.

Once the optimum conditions were established in preliminary tests, the deflocculation curve of slips containing 58 wt % HA was determined by measuring the slip viscosity at increasing dispersant concentrations.

The rheology of prepared slips was measured using a Bohlin V88 viscometer (Bohlin Reologi U.K. Ltd., UK) with a measuring system of concentric cylinders. The shear stress was recorded in a sweep of continuously increasing and decreasing shear rates. The viscosity values were derived from shear stress plots versus shear rates. Every sample was left to rest for approximately 1 min before the measurements were made in order to minimize the effect of previous shear history. An interval of 10 s between shear rate increments was selected. The shear stress value was measured and averaged over 5 s (integration time) at a given shear rate.

Foaming of hydroxyapatite suspensions

The foam generation procedure involved the addition of the foaming agent Tergitol TMN10 (Fluka Chemie) into the slurry. This material is a polyethylene glycol trimethylnonyl ether. The concentration of this substance was varied in order to produce different levels of foam. The slurry then was subjected to vigorous stirring by a double-blade mixer at a speed of ~900 rpm. The whole procedure of foam generation was conducted in a sealed glove box under a nitrogen atmosphere to avoid the presence of oxygen, which can inhibit the polymerization reaction.

Gelation of the foamed suspensions

The initiation of the polymerization process was performed using chemical initiation by the redox pair persulfate–diamine. This procedure involved the addition of an initiator (APS, Ammonium Persulfate, Aldrich Chemical Co.) and a catalyst (TEMED, N,N,N′,N′Tetramethyl ethylene diamine, Aldrich Chemical Co.) to the foamed suspensions. The catalyst, or reducing agent, was injected into the system and homogenized for a few seconds prior to addition of the initiator solution. After further stirring to homogenize the mix, the solution was cast by pouring it into a mold. A thermocouple probe was placed in the middle of the samples to monitor the exothermic polymerization reaction. The probe was connected to a data logger that recorded the temperature rise every 10 s. The polymerization procedure also was carried out in a sealed glove box at 0.0% oxygen.

Drying and firing

After polymerization took place, the foamed gels were allowed to cool down to room temperature before each sample carefully was removed from the container/mold. The samples were allowed to dry at room temperature for approximately 20 h. Further drying was conducted in an oven at 100°C for a minimum period of 10 h.

After drying the gelled bodies to eliminate the liquid solvent and machining, firing was performed in a high-temperature furnace using a heating rate of 1°C/min up to 300°C. This temperature was held for 90 min to complete burn-out of the organic components. The samples then were heated at a rate of 3°C/min up to the sintering temperature of 1250° or 1350°C, where they were held for periods of 2 h prior to cooling.

Characterization of the sintered foams

Using a diamond core-drill, the dried foams were machined into small cylinders measuring 15–16 mm in diam-

eter and height. The density and linear shrinkage was calculated using the dimensions and mass of the specimens in the green and sintered states.

In order to verify their phases before and after sintering, X-ray diffraction (XRD) was carried out using the initial powder and sintered foams crushed into powder.

Scanning electron microscopy (SEM) was performed to observe the pore morphology of the foams. As the material is nonconductive, nickel paint was applied to cover the lateral faces and edges of the foams, which then were gold coated for 4 min.

The compressive strength of porous specimens was measured using a material test system (MTS) universal testing machine at a cross-head speed of 0.05 cm/min. The specimens consisted of cylinders approximately 11–13 mm in diameter and height. The fracture stress was calculated using the failure load and the cross-sectional area of each specimen.

Cytotoxic evaluation

Cytotoxic evaluation of the sintered foams was performed in order to detect any changes in the toxicity of the material during processing. The method was carried out with a dilution of crushed hydroxyapatite extract in contact with a mammalian cell culture.[8] Phenol solution (0.02%) and alumina extract were used as a positive control (cytotoxic) and a negative control (noncytotoxic), respectively.

Quantities (6 g) of crushed sintered foam and of alumina powder were sterilized in an autoclave at 121°C for 20 min. Each of the samples had additions of 60 mL of the culture medium RPMI-FCS (RPMI 1640, containing 10% fetal calf solution and 1% penicillin/streptomycin solution). The mixtures were incubated for 48 h at 37°C. After this period, the supernatants were filtered and the extracts and 0.02% phenol solution were diluted with RPMI-FCS.

Chinese hamster ovary K-1 cells (CHO) from the American Type Culture Collection bank (ATCC - CHO k1) were cultured in RPMI-FSC medium at 37°C in a humidified 5% CO_2 air incubator. After a monolayer confluent propagation, 0.2% trypsin solution was added for detachment of cells from the container walls. The cell suspension was adjusted to a concentration of 100 cells/mL. Two mL were seeded to each 60-mm Petri dish and then were incubated for 5 h. After cell adhesion on the dishes, the culture medium was removed and replaced by 5 mL of pure medium and diluted extracts (100, 50, 25, 12.5, and 6.25%). Three samples of each extract dilution were made. Incubation was performed at 37°C and 5% CO_2 for 7 days. The medium then was removed, and the colonies formed were fixed with 10% formol in 0.9% saline solution and stained with Giesma. The visible colonies were counted on each plate and compared in number to the colonies present in the CHO control plate.

The cytotoxicity potential of the evaluated material was expressed as a cytotoxicity index (IC 50), which represents the extract concentration that suppresses 50% of the colony formation compared to the control.

RESULTS AND DISCUSSION

Powder morphology

The micrographs in Figure 1(a,b) show the morphology of the HA powder observed on the SEM and TEM, respectively. The powder is composed of clusters of submicron acicular crystallites. At increased magnification the crystal displayed lengths of approximately 0.1 μm and breadths of 0.02–>0.05 μm.

Powder dispersion

Dispersion experiments started with varying the powder concentration in the slips to maximize the loading of solids and to achieve control over the slip's rheology in order to enable easy foaming. It is known from previous work that the loading of high solids

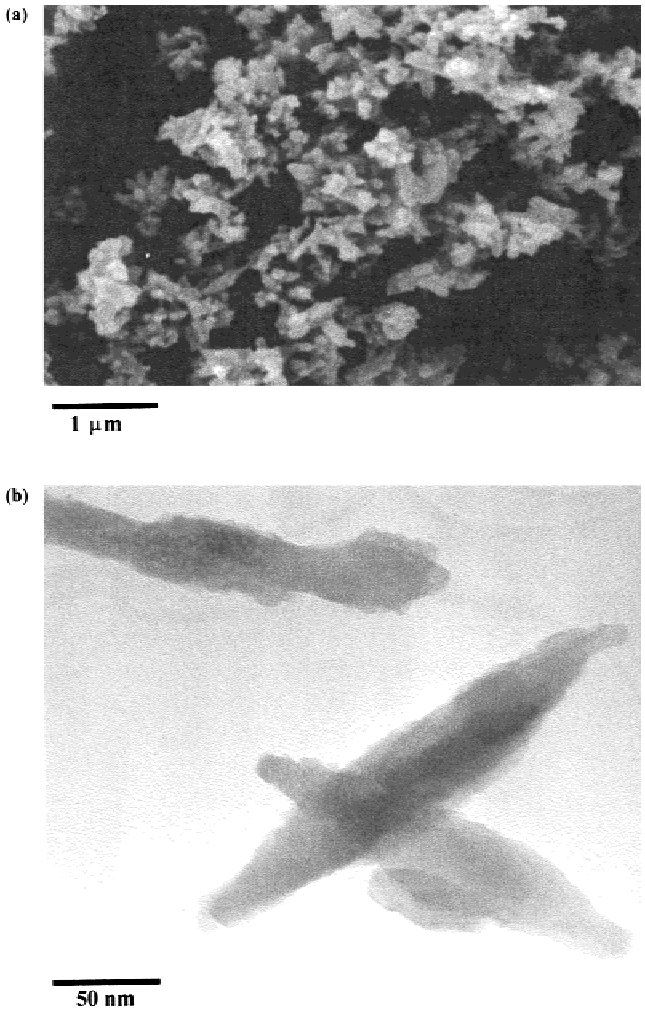

Figure 1. Morphology of HA powder under (a) SEM and (b) TEM observation.

affects the ability to produce large quantities of foam.[7] Nevertheless, this is desirable to reduce the shrinkage levels during drying and to increase the green density in the ceramic matrix. On the other hand, the loading of too low solids leads to low viscosity slips that form unstable foams. The latter suffer rapid collapse and result in gelled bodies with deteriorated structures. Hence a compromise exists between slip viscosity and foam volume properties that must be considered in the production of foamed suspensions.

Owing to its fine crystal size, intrinsically associated with large surface area, the HA powder was very difficult to disperse. The production of fluid suspensions was possible only at a low solids concentration, with a maximum 58 wt % powder (~30 vol %). Above this level slips exhibited viscosities higher than 1000 MPa.s at shear rates ranging between 0–1200 s^{-1}, which resulted in poor foaming.

Viscosity versus shear rate curves for slips of 58 wt % solids at increasing dispersant concentration are shown in Figure 2. At a dispersant concentration of 11.6 mg/g, the slips presented high viscosity levels and a certain pseudoplasticity. Other slips exhibited mainly a shear-thickening behavior, with lower levels of viscosity. This effect is probably caused by the release of the acicular crystals from agglomerates when a more dispersed state is achieved by the addition of polyelectrolytes. The needle shape of the particles provokes irregular packing and makes shearing more complex.

A minimum viscosity was achieved at 70 mg/g dispersant, as seen in Figure 2(b). This minimum was maintained within a very narrow range of dispersant concentration. A significant increase in viscosity took place above this level. The high content of dispersing agent necessary for dispersion has been noted for other materials also and has been attributed to the influence of monomers adsorbing onto the surface of the particles.[7]

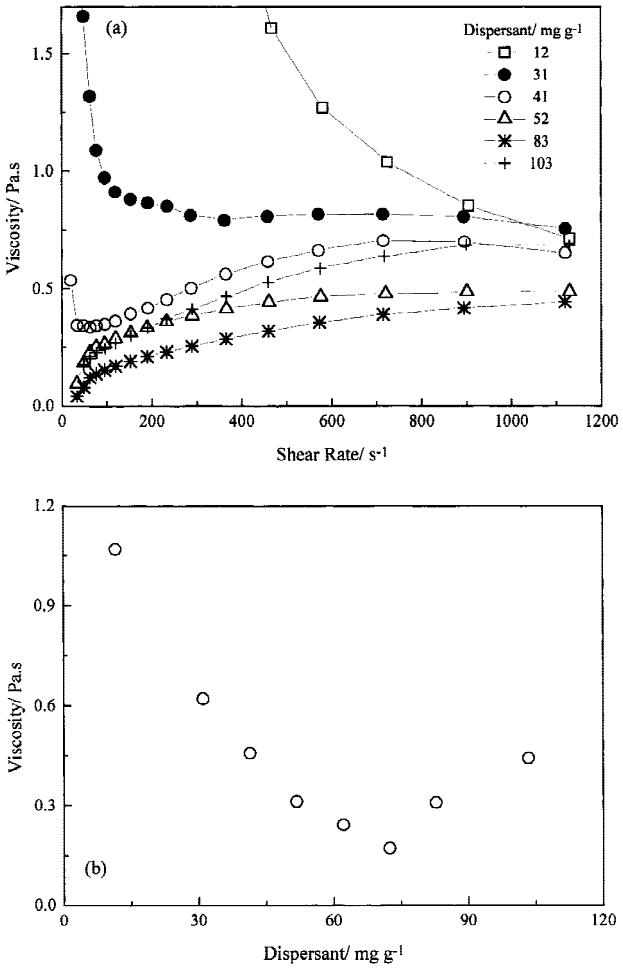

Figure 2. (a) Flow behavior of HA suspensions containing 58 wt % solids using polyacrylic acid as a dispersant in the indicated concentrations. (b) Deflocculation curves of 58 wt % HA slips measured at a constant rate of 450 s^{-1}.

Foaming and gelation

Foaming is in itself a simple process. It is based on the addition of surfactants to reduce the surface energy of liquid–gas interfaces as a means of generating stable bubbles.[9] Given that an appropriate foaming agent is employed, such as nonionic versions that do not interfere with the dispersion, foaming can be achieved without problems most of the time.

The foam volume varied according to the quantity of surfactant added, foams expanded during agitation reaching a maximum volume in approximately 4 min for the double-bladed shearer employed.

The high viscosity and shear-thickening behavior of the HA slurries caused some difficulties during foaming. Despite the quite high water content, only low foam volumes could be generated, even at high foaming agent concentrations. The shear-thickening behavior leads to a viscosity increase during foam generation that presumably opposes air entrapment and foam volume increase.

Gelation

The final, and possibly most important, requirement in determining the quality of the bodies produced is the stage of setting the foamed suspensions. Previous work in the literature has demonstrated that techniques other than *in situ* polymerization that employ a setting mechanism result in weak green bodies since the binder is not sufficient to retain a strong porous structure. However, the gel formed by *in situ* polymerization creates a three-dimensional polymeric network, which produces strong, machineable green bod-

ies. An efficient setting mechanism also insures the production of an homogeneous matrix with good particle packing.

Generally, the APS and TEMED concentrations used, in the range of 5–25 $\times 10^{-5}$ mol/g, led to highly exothermic reactions, and strong gelled bodies were produced. A typical gelation curve is shown in Figure 3. After addition of the reagents, the reaction initially is inhibited for a period known as the induction period, or idle time, after which the reaction proceeds and a temperature rise is observed. An ideal idle time is one that allows casting of the foam into the mold to be completed whereas too long an idle time is be avoided since collapse of the foam can take place. The concentration of reagents, temperature, pH, and the oxygen content in the system are known to affect the onset of polymerization.[10]

Drying and sintering

Typical problems associated with the drying stage, such as cracking and warping, were not observed in this process despite the fact that the water content in the slips was high. Interconnected porosity and high surface area are the factors that allow the solvent and binders to be removed with ease, contrary to what has been reported for the gel-casting of dense bodies.[11,12] Therefore the heating rates can be as fast as those employed in other processes, with no special attention required.

Sintering HA is important because in the same manner that high temperatures densify the microstructure and maximize the fracture strength, decomposition of the HA mineral phase also may take place. The appearance of other calcium phosphate derivatives is undesirable because they differ from HA in solubility and in strength and could result in problems with respect to the implant properties.

The HA powder used in this work revealed high stability at the sintering temperatures employed. The XRD patterns of the HA powder and of material sintered at 1250° and 1350°C are displayed in Figure 4. All three diffraction patterns show the peaks appropriate for the hydroxyapatite phase, demonstrating the high stability of the powder even at 1350°C. The patterns also were analyzed for traces of calcium phosphate; however, this phase was not detected. The high stability of the hydroxyapatite phase at temperatures around 1350°C is an interesting result. Several authors have reported the decomposition of HA powders into tricalcium phosphate (TCP) and tetracalcium phosphate at temperatures above 1150°C.[13] The high stability of the HA powder used in the present study was advantageous since fully densified pore walls were not obtained at the lower sintering temperature of 1250°C.

Post-sintering densities of 0.50 g/cm^3 and 0.69 g/cm^3 were obtained for green specimens of 0.36 g/cm^3 when the sintering temperature was 1250° and 1350°C, respectively. The corresponding linear shrinkages were 18 and 26%, respectively. Final porosity was 84.2 and 78.3%, based on the theoretical density of HA powder (3.16 g/cm^3).

The SEM micrographs in Figure 5 show the microstructure evolution during sintering. Temperatures of 1250°C were not sufficient to produce densified pore walls and struts. The under sintering state clearly can be seen in the micrographs. After sintering at 1350°C, densification occurred at high levels. The average grain size for these samples was 2–5 μm. In general, some residual porosity was revealed in the struts of sintered bodies at 1350°C as a result of poor particle packing during powder dispersion.

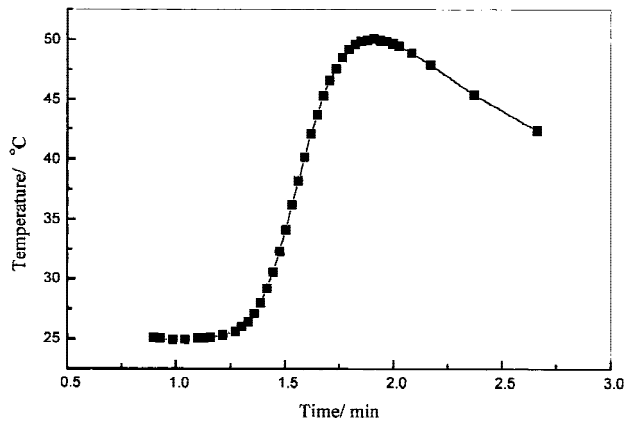

Figure 3. Typical gelation curve after addition of initiator and catalyst to promote polymerization of the organic monomers.

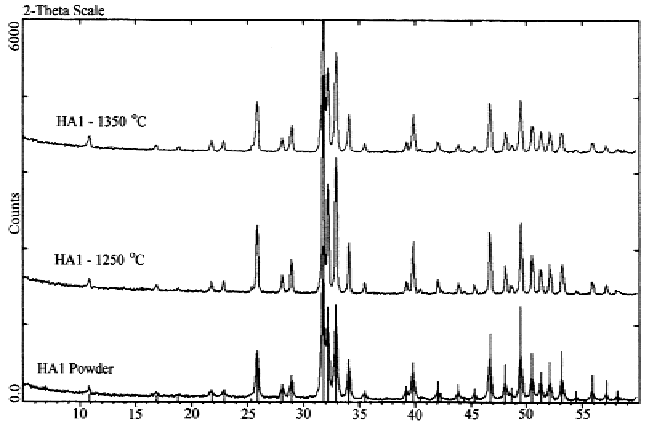

Figure 4. XRD pattern of HA powder in its original form (HA powder) and from foams sintered at 1250° and 1350°C. The only phase identified was hydroxyapatite.

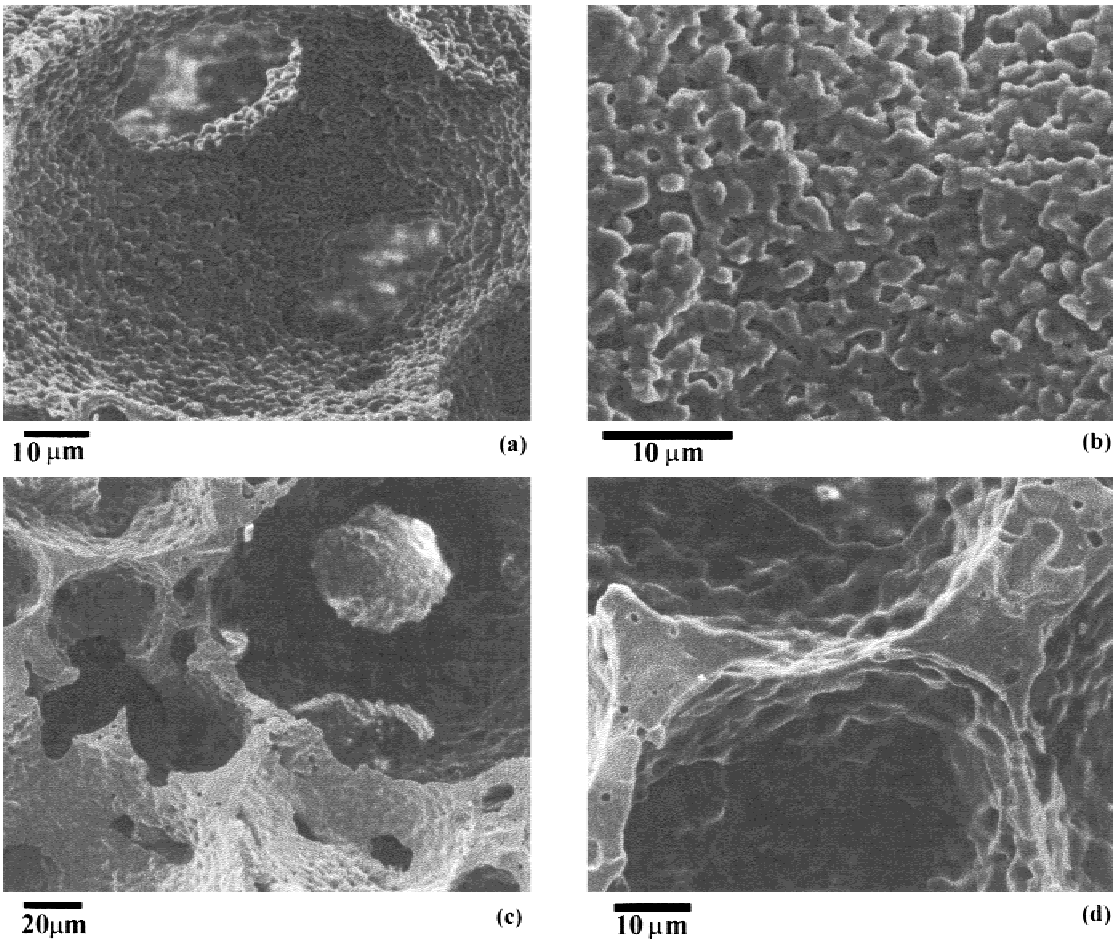

Figure 5. Evolution of the microstructure with sintering. SEM micrographs of HA foams having original green density of 0.36 g/cm^3 and sintered for 2 h at (a,b) 1250°C and (c,d) 1350°C.

Density and porosity

Once it was established that a sintering cycle of 1350°C for 2 h led to densified microstructures without decomposition of HA, these conditions were employed for other specimens. Thus bodies with green densities from 0.22 to 0.45 g/cm^3 were sintered and resulted in densities of 0.44 to 0.75 g/cm^3 (89.6 to 76.2% theoretical density).

The porosity volume varied according to the amount of surfactant added to the slips during the foaming process. In Figure 6, the density data are plotted as a function of foam volume generated. Errors in this measurement are large and generally can be explained by the deviation in foam volume that results due to the difficulty found in foaming.

The microstructural effects of density can be seen in Figure 7. The cell size in the foams becomes larger as the density is decreased. This difference is clear in the micrographs, where an average cell size range reveals a significant increase when the density decreases. For instance, porous bodies with 88% porosity generally have cell sizes larger than 200 μm in diameter whereas specimens with 80% porosity contain cells with a minimum diameter of 20 μm and a maximum of around 100–200 μm. Several factors can affect the cell size. These include the slip rheology, foam volume, type of surfactant used, the idle time prior to polymerization, and other mechanisms that may alter the process of bubble formation and coalescence.

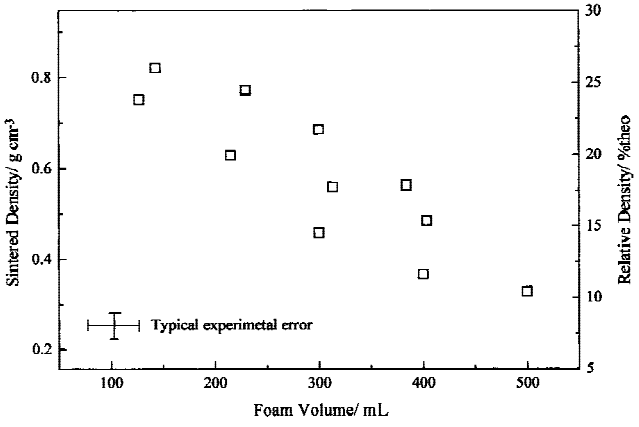

Figure 6. Sintered density of HA foams as function of the foam volume. Sintering at 1350°C for 2 h.

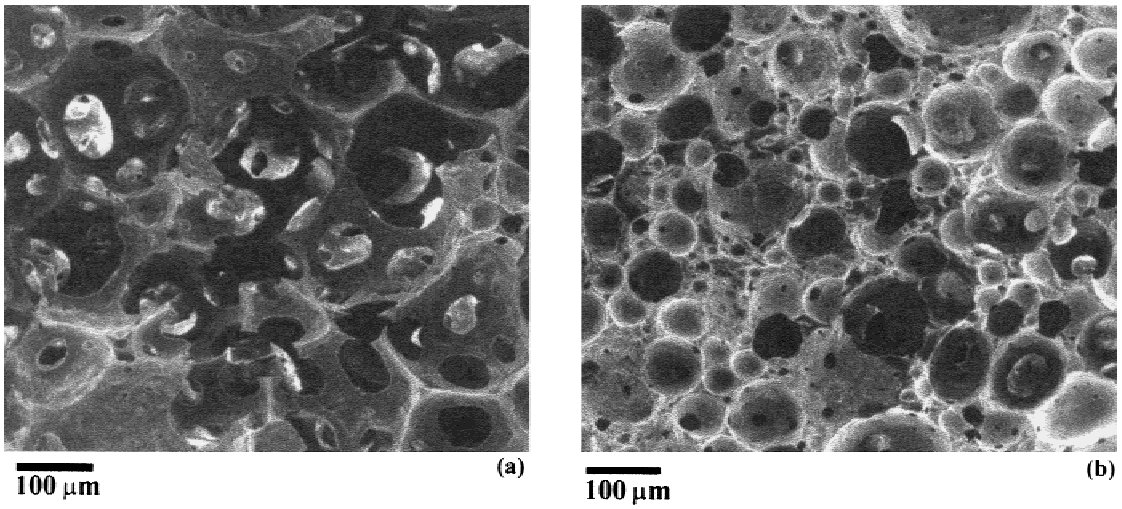

Figure 7. SEM micrographs illustrating the cell size distribution of HA foams at sintered densities of (a) 12% and (b) 20% theor.

Provided the slips are stable and well dispersed and that procedures for foaming and gelation can be executed without problems, the microstructures of the ceramic walls and struts appear to be uniformly distributed. This homogeneity must be preserved during drying, machining, binder burn-out, and sintering.

Compression strength

The compressive strength results are shown in Table I. While a degree of variation was observed, the strength levels obtained appear to be significantly higher than those typically observed in the literature for porous hydroxyapatite. For instance, data reported by Liu reveal compressive strengths lower than 2.5 MPa for bodies containing porosity higher than 70%.[14]

Cytotoxicity tests

The results of the *in vitro* test of cytotoxicity are shown in Figure 8. The values indicate the percentage of colonies formed in each Petri dish in relation to the CHO control dish against the concentration of the extracts. The cytotoxic potential can be quantitatively estimated from a projection of these data, as indicated in Figure 8. An index $IC_{50(\%)}$ represents the concentration of extracts that causes death of 50% of the cell population. As expected, the alumina (negative control) led to a noncytotoxic response ($IC_{50(\%)} > 100$) while the phenol solution (positive control) demonstrated a cytotoxic response with $IC_{50(\%)}$ of about 48. This index indicates that in a concentration of 48%, the phenol solution eliminated 50% of the cell population. The extracts prepared from porous HA revealed $IC_{50(\%)} > 100$, thus indicating the nontoxicity of the material.

The experiments show that the fabrication process used to produce the porous ceramics did not compromise the original purity of the biomedical-grade HA. In general, in products intended for implant applications, all substances incorporated must meet a high

TABLE I
Compressive Strength of Porous Hydroxyapatite Made From CAPTAL-R Powder

Density/g/cm^3	Porosity/%	Compressive Strength/MPa
0.61–0.63	80.2–80.7	4.4–4.7
0.74	76.7	7.4

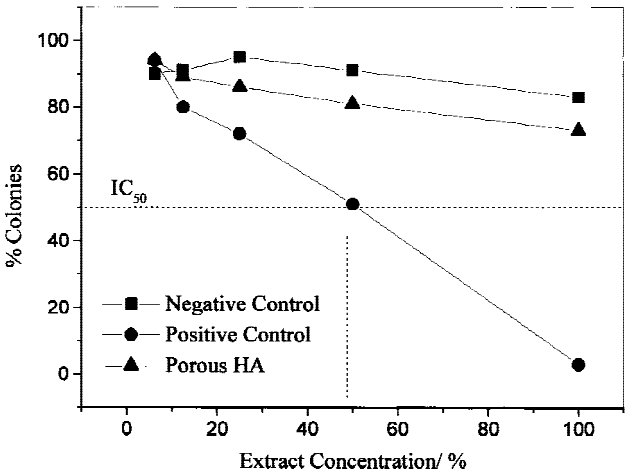

Figure 8. Test of cytotoxicity: Colony suppression curve of sintered HA foams.

standard of purity and must be completely eliminated in the firing process.

However, the results of these *in vitro* tests provide only the first requirement for these porous ceramics to be used as bone implants. Any implants also would have to fulfill criteria for biocompatibility, biofunctionality, and mechanical properties; for example, large pore size and large interconnecting windows between the pores enable faster bone growth in the region. Pore sizes larger than 200 μm have been reported to allow bone ingrowth.[15] The pore sizes resulting from our process tend to be a function of density but can be controlled to within the desired range. For example, large pore sizes can be achieved by expansion of the foams before gelation.

CONCLUSIONS

The current investigation has shown that a successful production of hydroxyapatite gel-cast foams can provide strong bodies with porosity as high as 90%.

Some difficulties with the dispersion of powders in aqueous systems that contain monomers may be found, which can affect the final foam volumes. Gelation generally proceeds without problems, however, assuming that an adequate reagent concentration is chosen. This results in uniform, strong foams that can be machined in the green form.

The structure of the pores is characterized by spherical and interconnected cells measuring 20 μm to 1 mm in diameter. Intrinsically, the cell size varies relative to the density of the specimens; however, methods for controlling the bubble size in the foams can provide the means for controlling the pore size.

Cytotoxicity tests demonstrated that the original biomedical purity of the HA powder is affected neither by the processing nor by the reagents used in the process. These results indicate that gel-cast porous HA can be considered as a potential candidate material for applications such as non-load-bearing bone implants. Further investigations are underway to evaluate the material in terms of biocompatibility and of adequate pore size for bone growth.

References

1. Liu DM. Porous hydroxyapatite bioceramics. In: Liu, DM, editor. Key engineering materials. Vol. 115. Uetikon-Zuerich, Switzerland: Trans Tech Publications; 1996, p 209–232.
2. Fabri M, Celotti GC, Ravaglioli A. Hydroxyapatite-based porous aggregates: Physico–chemical nature, structure, texture and architecture. Biomaterials 1995;16:225–228.
3. Arita IH, Wilkison DS, Mondragon MA, Castano VM. Chemistry and sintering behaviour of thin hydroxyapatite ceramics with controlled porosity. Biomaterials 1995;16:403–408.
4. Ioku K, Kurosawa H, Shibuya K, Yokozeki H, Hayashi T. *In vivo* reactions of the porous hydroxyapatite, β-TCP and β-TCP coated hydroxyapatite. In: Anderson OH, Yli–Urpo A, editors. Bioceramics vol. 7. Proceedings of the 7th International Symposium on Ceramics in Medicine, Turku, Finland, July 1994. Oxford: Butterworth–Heinemann Ltd. 446 p.
5. Constantino PD, Friedman CD. Synthetic bone graft substitutes. Craniofacial skeletal augmentation and replacement. Otolaryngol Clin N A 1994;27(5):1037–1074.
6. Sepulveda P. Gelcasting foams for porous ceramics. Ceram Bull 1997;76(10):61–65.
7. Sepulveda PAI, Binner JGP. Processing of cellular ceramics by foaming and in situ polymerization of organic monomers. J Eur Ceram Soc 1999;19:2059–2066.
8. International Standard: Biological evaluation of medical devices. Part 5. Tests for cytotoxicity: *In vitro* methods. ISO 1993; 10:993–995.
9. Rosen MJ. Foaming and anti-foaming by aqueous solutions of surfactants. In: Surfactants and interfacial phenomena. 2nd ed. New York: John Wiley & Sons, Inc.; 1989. p. 277–303.
10. Odian G. Principles of polymerization. 3rd ed. New York: John Wiley & Sons, Inc.; 1991. 768 p.
11. Janney MA, Omatete OO. Method for molding ceramic powders using water-based gel casting. US patent no. 5028362; 1991.
12. Young AC, Omatete OO, Janney MA, Menchhofer PA. Gelcasting of alumina. J Am Ceram Soc 1991;74(3):612–618.
13. Miquel JL, Facchini L, Legrand AP, Rey C, Lemaitre J. Solid state NMR to study calcium phosphate ceramics. Coll Surfaces 1990;45:427–433.
14. Liu DM. Influence of porosity and pore size on the compressive strength of porous hydroxyapatite ceramic. Ceram Int 1997;23:135–139.
15. Ravaglioli A, Krajewski A. Bioceramics: Materials, properties, applications. London: Chapman and Hall; 1992. 432 p.